Cell, Vol. 115, 151–162, October 17, 2003, Copyright ©2003 by Cell Press

TSH Is a Negative Regulator of Skeletal Remodeling

Etsuko Abe,[1,2] Russell C. Marians,[1] Wanqin Yu,[1,2] Xue-Bin Wu,[1,2] Takao Ando,[1] Yanan Li,[3] Jameel Iqbal,[1,2] Leslie Eldeiry,[1,2] Gopalan Rajendren,[1,2] Harry C. Blair,[3,4] Terry F. Davies,[1] and Mone Zaidi[1,2]

[1]Mount Sinai Bone Program
Department of Medicine
Mount Sinai School of Medicine
New York, New York 10029

[2]Veterans Affairs Medical Center
Bronx, New York 10463

[3]Department of Pathology
University of Pittsburgh
Pittsburgh, Pennsylvania 15213

[4]Veterans Affairs Medical Center
Pittsburgh, PA 15213

Summary

The established function of thyroid stimulating hormone (TSH) is to promote thyroid follicle development and hormone secretion. The osteoporosis associated with hyperthyroidism is traditionally viewed as a secondary consequence of altered thyroid function. We provide evidence for direct effects of TSH on both components of skeletal remodeling, osteoblastic bone formation, and osteoclastic bone resorption, mediated via the TSH receptor (TSHR) found on osteoblast and osteoclast precursors. Even a 50% reduction in TSHR expression produces profound osteoporosis (bone loss) together with focal osteosclerosis (localized bone formation). TSH inhibits osteoclast formation and survival by attenuating JNK/c-*jun* and NFκB signaling triggered in response to RANK-L and TNFα. TSH also inhibits osteoblast differentiation and type 1 collagen expression in a *Runx-2*- and osterix-independent manner by downregulating Wnt (LRP-5) and VEGF (Flk) signaling. These studies define a role for TSH as a single molecular switch in the independent control of both bone formation and resorption.

Introduction

Mammalian skeletal remodeling occurs throughout life whereby old bone that is resorbed by the osteoclast is replaced by new bone deposited by the osteoblast (Blair et al., 2002). The processes of resorption and formation are coupled tightly in a temporal and spatial sequence ensuring the maintenance of skeletal mass and integrity (Karsenty and Wagner, 2002). Osteoporosis, a major public health hazard worldwide, results from the loss of such temporal coupling (Manolagas and Jilka, 1995). Postmenopausal hypogonadism, a major cause of human osteoporosis, arises from osteoclastic activation triggering an increased resorption rate that is not fully compensated even by an accompanying increase in bone formation. Hyperthyroid states in both humans and animals similarly display a temporal uncoupling and hence a high remodeling bone loss (Greenspan and Greenspan, 1999). A different form of uncoupling occurs in Paget's bone disease. Here, bone formation dissociates both temporally and spatially from bone resorption and becomes rapid, autonomous, and disorganized. This results typically in focal osteosclerosis characterized by disordered collagen deposition and the formation of woven, as opposed to lamellar bone, sometimes at unresorbed sites.

Physiologic mechanisms controlling skeletal remodeling have unraveled only recently through the application of genetic manipulation. It is clear that molecules that are necessary for either bone formation or bone resorption, when deleted, produce an overt skeletal phenotype. Thus, osteoblast formation is abrogated in *Runx-2*- or osterix-deficient mice (Karsenty and Wagner, 2002). Likewise, profound osteopetrosis due to absent osteoclast formation ensues when M-CSF, c-*fos* or RANK-L are absent (for review, see Zaidi et al., 2003). In contrast, seemingly important resorption activators, such as interleukin-6 and tumor necrosis factor-α that markedly affect bone cells in vitro, when deleted in mice, do not produce osteopetrosis. Similarly, not many osteoclast inhibitors cause an accelerated resorption when deleted, likely because of degenerate mechanisms designed to prevent excessive skeletal loss. Even the deletion of both estrogen receptors α and β, together, produces not as pronounced a phenotype as would be expected from estrogen's in vitro action (Sims et al., 2003). Thus, for its deficiency to result in profound bone loss, a given molecule must not only be necessary for skeletal maintenance, but must also overcome compensation and redundancy (Zaidi et al., 2003).

The only established biologic function of thyroid stimulating hormone (TSH) is to regulate the synthesis and secretion of thyroid hormone from thyroid follicular cells. Here, it interacts with a seven transmembrane, glycosylated G protein-coupled TSH receptor (TSHR). It has been shown through binding studies and immunodetection that cells and organs other than the thyroid, including lymphocytes, the pituitary, thymus, testes, kidney, brain, adipose tissue, and fibroblasts express TSHRs (for review, see Davies et al., 2002). Several biological roles for TSH have thus been speculated. For example, TSH is thought to play a role in recruiting intestinal epithelial lymphocyte subsets to the gut (Wang and Klein, 1995). TSHRs on preadipocytes are thought to induce lipolysis and a thermogenic response (Valyasevi et al., 1999). Likewise, TSHRs in anterior pituitary folliculo-stellate cells have been implicated as ultra short loop regulators of TSH production itself (Kohn et al., 1995). And, finally, in astrocytes throughout the brain, as well as in neurons of the hypothalamus, hippocampus, and pyriform and postcingulate cortices, TSH may regulate the hypothalamic-pituitary axis (Prummel et al., 2000). For none of these actions, however, has TSH been shown to be either necessary or sufficient.

TSH has never been shown to have physiologically

*Correspondence: mone.zaidi@mssm.edu

relevant effects on bone or bone cells. The osteoporosis of human hyperthyroidism that is associated with low or undetectable TSH levels has traditionally been attributed instead to elevated thyroid hormone (T_3 and T_4) levels. Likewise, the high bone mass accompanying the elevated TSH in hypothyroidism is thought to result from low thyroid hormone levels. There is indeed a substantive body of early literature on the effects of thyroid hormones on bone remodeling, both resorption and formation, in vitro (Bordier et al., 1967; Sato et al., 1987; Britto et al., 1994). Nonetheless, remodeling is not uncoupled in mice lacking the α_1 and β thyroid hormone receptors (TRs). These mice instead display skeletal morphogenesis and growth plate abnormalities (Gothe et al., 1999). That $\alpha 1/\beta$ TR deficiency essentially produces no remodeling phenotype prompted us to speculate that the osteoporosis and the increased bone mass seen, respectively, in hyper- and hypothyroidism could potentially arise from altered TSH levels.

Thus, we attempted, in this study, to examine for direct, hitherto unknown effects of TSH on bone remodeling using complementary cellular and molecular approaches, notably through the use of TSHR null mice. We demonstrate that even a 50% reduction in TSHRs in euthyroid mice results in pronounced osteoporosis and focal osteosclerosis, that TSHRs are abundant on both osteoclast and osteoblast precursors and that TSH negatively regulates both osteoclastic bone resorption and osteoblastic bone formation by attenuating distinct signals. The data thus implicate TSH as a single necessary molecular switch that negatively regulates both components of skeletal remodeling.

Results

TSHR Knockout Mice Display High Turnover Osteoporosis and Focal Osteosclerosis

Our group generated TSHR null mice by deleting exon 1 of the mouse TSHR gene through homologous recombination in embryonic stem cells and replacing it with a GFP cassette (Marians et al., 2002). GFP expression, in lieu of gene deletion, allowed us to examine TSHR localization in situ. Intense GFP fluorescence was detected in thyroid follicles of $TSHR^{+/-}$ and $TSHR^{-/-}$ mice. Thyroid follicles were poorly developed in $TSHR^{-/-}$ mice, not unexpectedly, as follicular growth and differentiation are TSH-dependent. Western blots of thyroid homogenates showed an expected 50% decrease of TSHR expression in the heterozygotes and an absent expression in TSHR null mice.

TSHR null mice were runted, hypothyroid, and died by 10 weeks of age. Body weight and femur length and weight were all reduced (Table 1). Serum T_3 and T_4 levels were undetectable and TSH levels were elevated several thousand-fold. In contrast, the heterozygotes thrived and reproduced normally with normal serum T_4, T_3, and TSH levels (Table 1). Dietary supplementation of $TSHR^{-/-}$ mice with thyroid extract (100 ppm) at weaning normalized body weight, but not bone weight or bone length (except femur weight) (Table 1). Serum calcium levels were normal in all groups.

TSHR null mice had severe osteoporosis at all sites as assessed by Piximus-based bone mineral density (BMD) measurements (Figure 1A). Even the heterozygotes with normal circulating T_4 and T_3 levels showed a significant BMD reduction ($p < 0.01$). Thyroid extract supplementation to TSHR null mice did not normalize the BMD change (Figure 1A) confirming that the bone loss was independent of T_3 and T_4 levels. Histomorphometry revealed significant increases in TRAP-labeled surfaces in vertebral bodies of $TSHR^{-/-}$ mice, suggestive of increased osteoclastic bone resorption (Table 2). Finally, calvarial thickness was reduced significantly in the supplemented $TSHR^{-/-}$ mice compared with wild-type littermates ($p < 0.01$) (Figure 1B).

In addition to the systemic bone loss despite normal calcium, TSH and T_3/T_4, there was increased bone turnover with increased woven bone in both heterozygotes and null mice. In thyroid-replaced, TSHR-deficient mice this increase in bone turnover was dramatic. High turnover states typically show variability in BMD, and, despite overall decreases in BMD (Figure 1A), irregular cortical thickening occurred in idiosyncratic locations in long bones (Figure 1C). Histology of vertebral cancellous bone showed disorganized trabeculae resembling Pagetic bone (Figure 1D) with significant increases in mean trabecular width in $TSHR^{-/-}$ mice (Table 2). Woven bone, the characteristic of rapid bone formation, was seen by polarization microscopy to be increased in all areas. In recently formed cortical bone, it was often difficult to detect lamellar bone in null mice, where control bone was entirely lamellar (Figure 1E, lower images). In keeping with these observations, calcein double-labeling studies in $TSHR^{-/-}$ mice showed that mineralizing surfaces increased ~50% with normal interlabel distances (Table 2).

To examine the cellular basis of the osteoporosis and focal sclerosis, we compared both osteoclast and osteoblast formation ex vivo in bone marrow cultures (see Experimental Procedures). Osteoclast formation was increased by ~2-fold in cultures from $TSHR^{-/-}$ and $TSHR^{+/-}$ mice compared to wild-type cultures (Figures 2A–2D). This was associated with a marked increase in expression of the osteoclast markers TRAP and the calcitonin receptor (Figure 2E). Likewise, colony forming unit-fibroblast (CFU-F) and colony forming unit-osteoblast (CFU-OB) counts were increased in stromal cell cultures from $TSH^{+/-}$ and $TSH^{-/-}$ mice compared with wild-type cultures (Figure 2F–2M). The increase in osteoblast differentiation in TSHR null and heterozygote mice was associated with enhanced expression of type 1 collagen, bone sialoprotein (BSP), and osteocalcin both in CFU-F colonies and long bone extracts (Figures 2N and 2O). That a prominent cellular phenotype was evident despite only a 50% reduction in the TSHR content suggests an important skeletal effect of TSH.

Bone Cell Precursors Express TSHRs

High-resolution dual photon confocal imaging showed GFP fluorescence in cells that resembled osteoblast and osteoclast precursors in the inner skull table (Figure 3A). Intense GFP fluorescence was also observed ex vivo in CFU-Fs at day 10 and in mononucleated osteoclast precursors at day 6 (Figure 3B). Quantitative FACS analysis showed a dramatic increase in GFP-expressing cells following RANK-L and M-CSF exposure (Figure 3C). The temporal sequence of TSHR expression, examined by immunostaining, coincided with calcitonin receptor ex-

Table 1. Phenotypic Features of the TSHR Null Mouse

	+/+	+/−	−/−	−/−(TH)
Body weight (g)	20.1 ± 1.2	23.6 ± 0.5	14.1 ± 1.1*	22.8 ± 0.9
Femur length (cm)	1.40 ± 0.04	1.38 ± 0.03	1.25 ± 0.03*	1.18 ± 0.03
Femur weight (mg)	76.0 ± 4.0	79.0 ± 6.0	62.0 ± 6.0*	72.0 ± 6.0
T4 (mg/dl)	4.0 ± 0.6	6.8 ± 0.8	ND	4.2 ± 0.7
T3 (ng/dl)	80.4 ± 4.0	78.8 ± 3.8	ND	93.0 ± 5.0
TSH (mU/ml)	61.5 ± 7.4	83.8 ± 8.8	31,000*	75.4 ± 3.8
Calcium (mg/dl)	9.7 ± 0.3	9.7 ± 0.5	NT	9.8 ± 0.3

The results are shown as means ± standard error of the means. Statistics: analysis of variance for each variable comparing heterozygote (+/−) or null (−/−) mice with or without thyroid extract (TH) supplementation to wild type (+/+) littermates. *$p < 0.01$. ND: not detectable. NT: not tested.

pression (day 2), but preceded TRAP expression (day 3) (Figure 3D).

RT-PCR on mRNA isolated from osteoclast precursor and CFU-F colonies displayed expected bands in wild-type mice, but not in TSHR null mice (Figure 3E). TSHR protein expression was confirmed in the same cultures by FACS using a murine monoclonal antibody RSR-1 raised to the human TSHR (epitope: amino acids 381–385, β subunit, kindly provided by Dr. Smith, FIRS Laboratories, Cardiff, UK) (Figure 3F). Finally, the osteoclast precursor cell line, RAW-C3, as well as, for comparison, CHO-cells transfected with either human or murine TSHRs (Ando et al., 2002), specifically bound ^{125}I-TSH (Figure 3G). Limited expression of TSHR was also noted in UAMS-33 preosteoblasts (Lecka-Czernik et al., 1999) using both RT-PCR and FACS (data not shown). Together, these findings indicate that TSHR expression is maximal during the early and mid phases of osteoclast and osteoblast formation.

TSH Regulates Osteoclast Formation, Function, and Fate

Ficoll-purified hematopoetic stem cells were cultured for 6 days with RANK-L and M-CSF in the presence

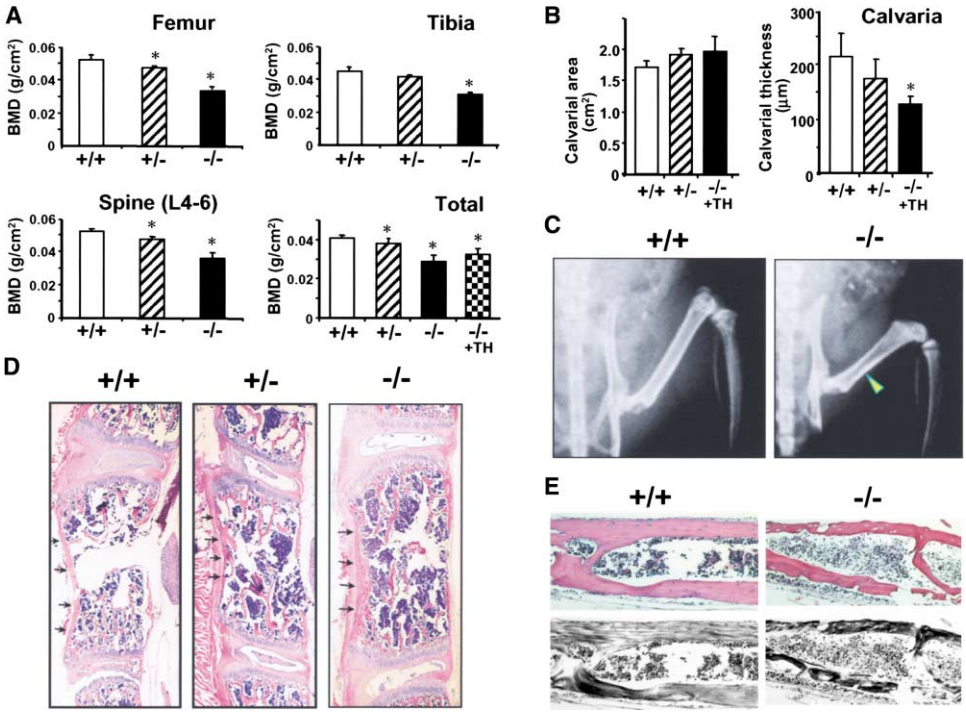

Figure 1. Osteoporosis and Focal Sclerosis in the TSH Receptor (TSHR) Knockout Mouse

(A) Reduced bone mineral density (BMD) in TSHR$^{-/-}$ and TSHR$^{+/-}$ mice. A Piximus (Lunar) small animal bone densitometer was used to measure bone mineral density (BMD) at the indicated sites. Of note is that supplement of dietary thyroid tissue extract (TH), rendering TSHR$^{-/-}$ mice euthyroid (Table 1), failed to reverse the osteoporotic phenotype.

(B) Calvarial area (cm^2) and thickness (μm) at parietal plate in the mid region, measured through digital image analysis. Statistics for (A) and (B): comparisons with wild-type littermates by analysis of variance; *$p < 0.01$.

(C) Microradiographs of TSHR$^{-/-}$ and TSHR$^{+/+}$ mice indicating areas of focal radioopacities (arrow).

(D) Hematoxylin-eosin staining of corresponding vertebral bodies from TSHR$^{-/-}$ and TSHR$^{+/-}$ mice and wild-type littermates, indicating focal sclerotic areas by arrows (magnification × 20).

(E) Hematoxylin-eosin staining (upper images) and corresponding polarized micrographs (lower images) showing the disorganized collagen orientation (woven bone) in TSHR$^{-/-}$ mice compared with normal lamellar collagen orientation in wild-type littermates.

Table 2. Bone Histomorphometry of the TSHR Null Mouse

Bone and Parameter (units) [Abbreviation]	+/+	+/−	−/−
Tibia, Diaphysis			
Cortex (μm) [Ct.Wi]	112 ± 6	103 ± 7	98 ±10
Vertebra, L3			
TRAP labeled surface (%) [OC.S]	20.9 ± 3.0	22.3 ± 2.9	31.1 ± 3.8*
Trabecular width (μm) [Tb.W]	23.1 ± 1.7	26.8 ± 1.5*	27.9 ± 1.6*
Mineralizing surface (%) [(dLS + sLS/2)/BS]	18.7 ± 4.7	22.7 ± 12.4	30.2 ± 7.0*
Interlabel distance (μm) [Ir.L.Th]	21 ± 3	22 ± 3	23 ± 4
Bone area (mm^2) [B.Ar]	2.0 ± 0.2	1.9 ± 0.2	1.8 ± 0.3
Trabecular Bone Area (TBA = BA/TA)	25.7 ± 2.0	23.8 ± 1.08	19.1 ± 1.4*

Histological measurements and calculated parameters in cortex and cancellous bone of 6-week-old, calcein-labeled, wild type (+/+), heterozygotic (+/−), and null (−/−) mice. Mineralizing surface is corrected for total surface; other measurements are from trichrome or von Kossa stained undecalcified or hematoxylin and eosin decalcified stained sections by digital measurements of photomicrographs as described. Nonstandard units are as defined by Parfitt et al., 1987. In vivo and ex vivo osteoclast labeling used the method of Webber et al., 1988. Mean ± standard deviations for cross sections from six animals per group. *Different from wild type $p < 0.05$.

of recombinant human TSH (rhTSH). rhTSH caused a concentration-dependent inhibition of osteoclast formation (Figure 4A). RAW-C3 cells were cultured in parallel with RANK-L for 6 days with or without rhTSH (10 U/l). TSH inhibited the osteoclastogenic effect at every RANK-L concentration (Figure 4B). This was associated with an inhibition of the RANK-L-induced stimulation of osteoclast markers, namely TRAP, cathepsin K, calcitonin receptor, and β_3 integrin measured by real-time PCR (Figure 4C).

We next compared resorption of dentin slices by osteoclasts derived from $TSHR^{-/-}$, $TSHR^{+/-}$, and $TSHR^{+/+}$

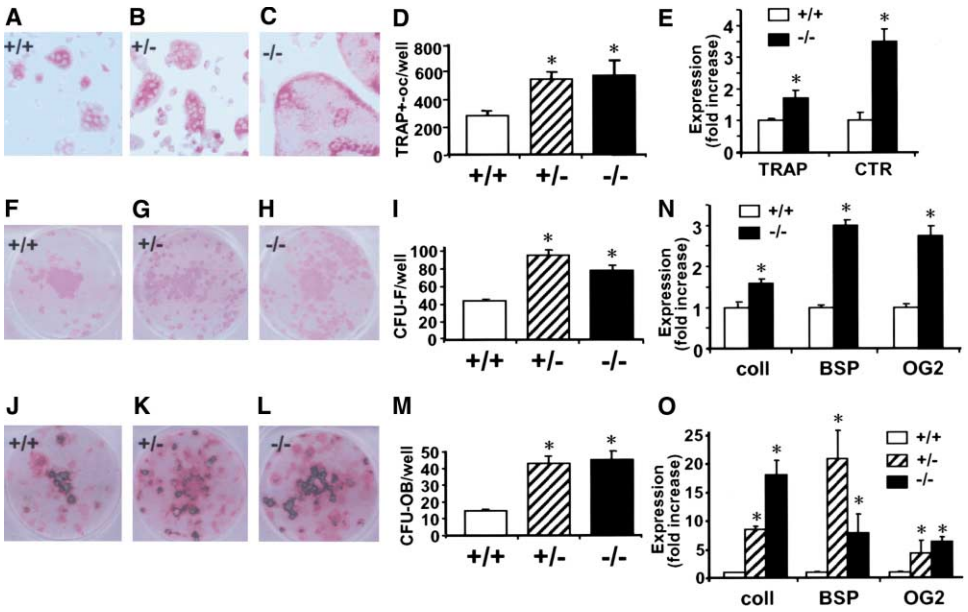

Figure 2. Effect of TSHR Deletion on Osteoblast and Osteoclast Formation in Bone Marrow Cell Cultures

Bone marrow cells were isolated from 6-week-old $TSHR^{+/+}$, $TSHR^{+/-}$, and $TSHR^{-/-}$ mice. Ficoll-separated hematopoetic stem cells were cultured with RANK-L (60 ng/ml) and M-CSF (30 ng/ml) allowing for the formation of TRAP-positive osteoclasts (A–D). TRAP and calcitonin receptor (CTR) mRNA expression (fold increase) was quantitated by real-time PCR (E). The stromal cell fraction was allowed to differentiate in ascorbic acid-2-phosphate (1 mM) to form alkaline phosphatase-positive fibroblastoid colonies, CFU-Fs, at day 10 (F–I), and mineralized von Kossa-positive colonies, CFU-OBs, around 21 days (J–M). Bone sialoprotein (BSP), type I collagen (coll), and osteocalcin (OG2) mRNA expression was quantitated by real-time PCR in CFU-Fs (Figure 2N) and long bones (Figure 2O), and is expressed as a fold increase (wild-type). Statistics by analysis of variance compared with the wild-type littermates, *$p < 0.01$.

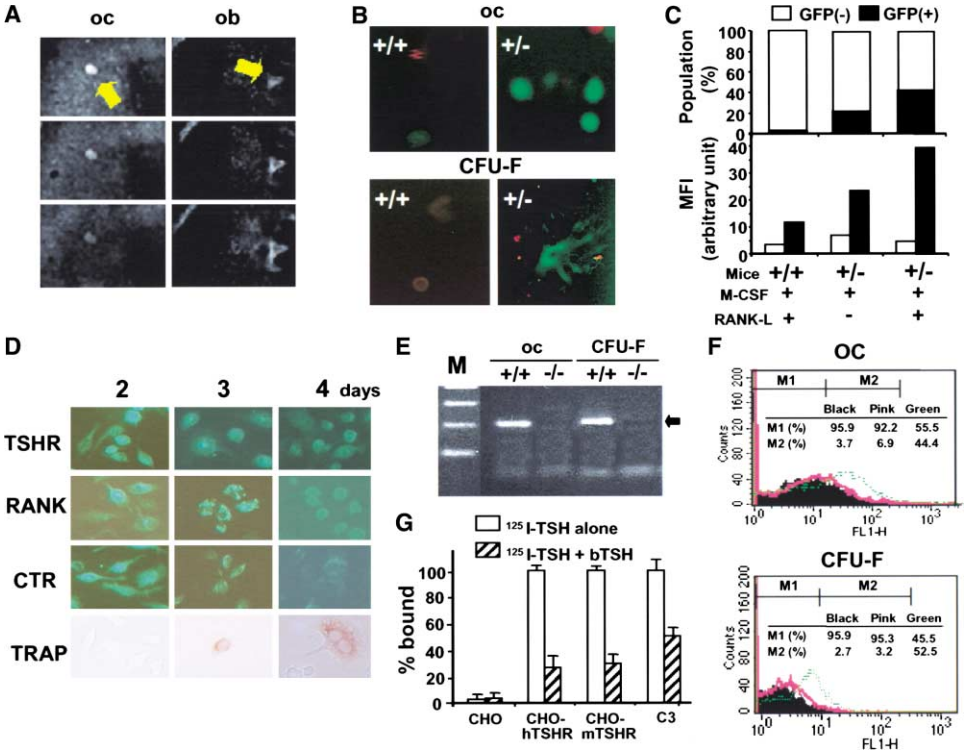

Figure 3. Expression of the TSHR in Bone Cells

(A) Dual photon confocal micrographs of calvaria from TSHR$^{-/-}$ mice showing GFP fluorescence from an osteoclast precursor (oc) and an osteoblast precursor (ob).

(B) Upper image: GFP expression in mononuclear osteoclast precursors (oc) following 6 day culture of Ficoll-purified hematopoetic stem cells from TSHR$^{+/-}$ and TSHR$^{+/+}$ mice with M-CSF (30 ng/ml) and RANK-L (60 ng/ml). No intense GFP fluorescence in control (TSHR$^{+/+}$) cultures. Lower image: GFP expression in colony forming units-fibroblasts (CFU-F) colonies formed after a 10 day incubation of bone marrow stromal cell cultures from TSHR$^{+/-}$ and TSHR$^{+/+}$ mice in differentiating conditions (1 mM ascorbic acid-2-phosphate).

(C) FACS quantitation of GFP fluorescence in hematopoietic stem cell cultures incubated with RANK-L and/or M-CSF, as above. MFI-mean fluorescence intensity of GFP-negative (open column) and GFP-positive (filled column) cells.

(D) Immunodetection of TSHR, RANK, and calcitonin receptors (CTR) and tartrate-resistant acid phosphatase (TRAP) staining during osteoclastogenesis in bone marrow cell cultures from wild-type mice (see Experimental Procedures for details).

(E) RT-PCR evidence for TSHR expression in osteoclast precursors (oc) and osteoblast precursors (CFU-Fs), cultured as described above, from wild-type and TSHR$^{-/-}$ mice. Lane M: markers. Arrow: 203 bp.

(F) TSHR protein expression in osteoclast precursors (oc) and CFU-F colonies from wild-type mice analyzed by FACS. Percent cells in the M1 and M2 zones are indicated. Black: no added antibody; red: goat antimouse IgG (0.4 μg/ml); green: mouse antihuman TSHR (RSR-1) antibody (10 μg/ml) followed by goat antimouse IgG (0.4 μg/ml). Note the spectral shift of the green zone toward M2 indicating protein expression.

(G) Specific ^{125}I-TSH binding to intact CHO cells, CHO cells transfected with murine (m) or human (h) TSHR, and RAW-C3 (C3) cells. Cells were incubated with 10,000 cpm of ^{125}I-bTSH in the absence or presence of cold bTSH (10^6 mU/l), and radioactivity in the cell lysates was counted. The binding of the ^{125}I-bTSH was expressed as a % bound in each cell line. The values are average of the quadruplicate samples.

following a 6 day incubation with RANK-L and M-CSF in the presence or absence of rhTSH (10 U/l). Resorption, quantitated as the number of pits per slice, was increased significantly in TSHR$^{-/-}$ cultures compared with wild-type cultures (Figure 4D). Expectedly, TSH inhibited resorption by wild-type, but not of TSHR$^{-/-}$ osteoclasts (Figure 4D).

Finally, we investigated whether TSH attenuated the lifespan of osteoclast precursors and mature osteoclasts. Otherwise TSHR-negative RAW264.7 cells were infected with a retroviral vector containing the hTSHR gene and protein expression was confirmed by FACS (Figure 5A). TSHR-infected cells became annexin V-positive when treated with TSH, whereas those infected with vector alone, or those not exposed to TSH did not (Figure 5B). All groups of cells showed similar (minimal) levels of propidium iodide uptake, indicating largely intact cell membranes (Figure 5B). Cell number in infected cells was reduced by ~15% ($p < 0.05$). In separate experiments, TSH stimulated apoptosis in mature osteoclasts derived from RAW-C3 cells (Vincent et al., 2001) in a concentration-dependent manner, maximally by ~50% (Figure 5C). Together, the results suggest that TSHR activation by TSH results in attenuated osteoclast formation, resorption, and survival.

TSHR Attenuates Osteoclastogenesis by Inhibiting JNK/c-*jun* and NFκB Signaling

It was necessary to differentiate whether the increased osteoclastogenesis in TSHR knockout mice arose from activated osteoclast precursors or whether it was secondary to enhanced RANK-L or M-CSF production from the osteoblast. Basal and 1,25-dihydroxyvitamin D_3-stimulated RANK-L or M-CSF expression in cultured

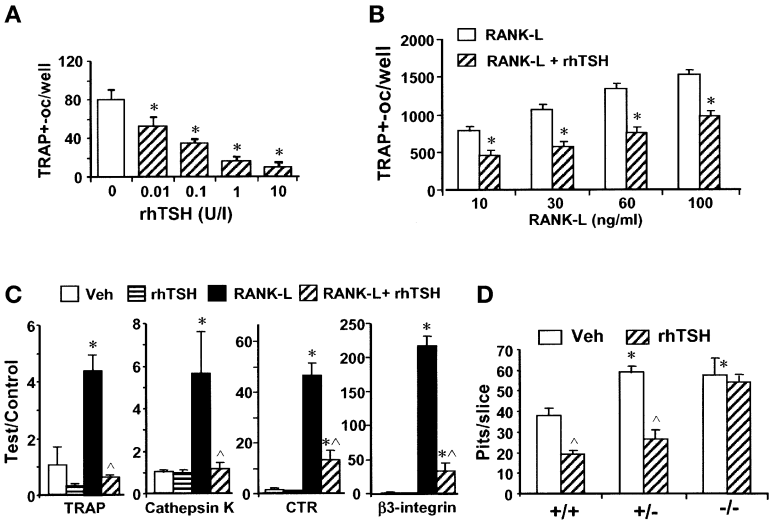

Figure 4. TSH Effects on Osteoclast Formation

(A) Inhibitory effect of recombinant human (rh) TSH on the formation of TRAP-positive osteoclasts. Hematopoetic stem cells were cultured with RANK-L (60 ng/ml) and M-CSF (30 ng/ml) allowing for osteoclast formation. Statistics: analysis of variance, *$p < 0.01$, comparison of each concentration with zero concentration.

(B) Effect of rhTSH (10 U/l) on osteoclast formation from TSHR-positive RAW-C3 cells incubated with various concentrations of RANK-L. Statistics: Analysis of Variance, $p < 0.01$ – RANK-L alone versus RANK-L+rhTSH.

(C) Expression of osteoclast markers, notably TRAP, cathepsin K, calcitonin receptor (CTR), and β_3 integrin in response to RANK-L stimulation with or without rhTSH (10 U/l). Statistics: analysis of variance, *$p < 0.01$–vehicle (Veh) versus treatment; ^$p < 0.01$ RANK-L alone versus RANK-L+rhTSH.

(D) Effect of rhTSH (10 U/l) or vehicle (Veh) on resorption (pits per slice) by osteoclasts generated from bone marrow derived from TSHR$^{-/-}$, TSH^{+}/$-$, and wild-type littermates (per Takahashi et al., 2003). Statistics: analysis of variance, $p < 0.01$, *comparison with TSHR^{+}/+ (untreated), ^control versus rhTSH-treated.

calvarial osteoblasts derived from TSHR null or heterozygote mice was not elevated compared with wild-type littermates (Figure 6A). In fact, basal RANK-L expression was reduced in TSHR$^{-/-}$ mice. This indicated that loss of the TSHR did not elevate osteoclast formation through increased RANK-L or M-CSF expression.

We found that TNFα, but not IL-7 levels in the supernatant of freshly isolated bone marrow cells measured by ELISA were higher by ~3-fold in TSHR$^{-/-}$ mice (Figure 6B). This increase in TNFα expression was confirmed by real-time PCR in cultured bone marrow cells (Figure 6B). We next examined whether the elevated TNFα caused the increased osteoclastogenesis in TSHR$^{-/-}$ mice. Excess anti-TNFα neutralizing antibody blocked this increase in osteoclast formation (Figure 6C), providing compelling evidence for TNFα as an osteoclastogenic signal mediating the effects of TSHR deletion.

The interaction of TNFα and (or) RANK-L with their receptors results in the binding of TNF receptor associated factors (TRAFs) to their respective intracellular domains and the subsequent activation of Akt, MAP kinases (JNK, ERK, and p38) and NFκB (Khosla, 2001; Teitelbaum and Ross, 2003). JNK, by phosphorylating c-*jun* at the N terminus, causes its nuclear translocation followed by the binding of homo- and heterodimeric complexes between c-*jun* and c-*fos* to AP-1 sites on gene promoters, including those of cathepsin K and TRAP (Kawaida et al., 2003). Likewise, the two subunits of NFκB, p65 and p50, are osteoclastogenic, and their nuclear translocation is inhibited by dephosphorylated IκBα. As phosphorylated IκBα is degraded through ubiquitination, inhibition of such phosphorylation by TSH could make more dephosphorylated IκBα available for binding to, and thus decreasing the nuclear translocation of the NFκB heterodimers.

Consistent with our premise that upregulated TNF signaling underlies the increased osteoclastogenesis in the TSHR$^{-/-}$ mouse, we found that steady-state levels of phosphorylated JNK and IκBα were increased in osteoclasts derived from TSHR$^{+/-}$ and TSHR$^{-/-}$ mice compared with those derived from wild-type littermates (Figure 6D). To examine the downstream mechanism further, we used TSHR-positive RAW-C3 cells. Apart from causing modest increases in ERK1/2 and p38 phosphorylation (data not shown), TSH potently inhibited basal and RANK-L-stimulated JNK and IκBα phosphorylation (Figures 6E and 6F). It likewise attenuated both basal and RANK-L-induced c-*jun*, but not c-*fos* translocation (Figure 6G). Finally, TSH inhibited RANK-L-induced nuclear translocation of p65 (Figure 6G). The latter mechanism, we believe, constitutes a parallel pathway through which TSH likely impairs osteoclast formation.

TSH Regulates Osteoblast Differentiation by Attenuating LRP-5 and Flk-1 Expression

Stromal cells derived from bone marrow were allowed to differentiate in ascorbic acid-2-phosphate ("differentiating conditions"). Within 10 days, adherent fibroblastoid colonies, CFU-Fs, formed that later mineralized, at around 21 days, to form CFU-OBs (Figure 7). TSH inhibited CFU-F and CFU-OB colony formation in a concentration-dependent manner (Figures 7A and 7B).

We used two model systems to study the mechanism of the inhibitory effects of TSH on osteoblast differentiation. First, primary osteoblasts isolated by collagenase digestion from calvaria of 4-day-old mice were cultured in differentiating conditions. Second, 1-day-old calvarial explants were maintained in culture with 1% agarose under differentiating conditions (Gong et al., 2001). In both systems, TSH (10 U/l) was applied for the entire 6 day culture period. Real-time PCR was employed on RNA extracted from cells or calvarial explants to examine the expression of the osteoblast markers type 1 collagen, BSP and osteocalcin, the critical transcription factors *Runx*-2 and osterix, and the prodifferentiation receptors LRP-5 and Flk-1 (Karsenty and Wagner, 2002). LRP-5, the coreceptor involved in Wnt signaling, promotes osteoblast differentiation and its mutation or deletion is associated with severe osteoporosis (Gong et al., 2001). Likewise, Flk-1, a VEGF receptor, is critical

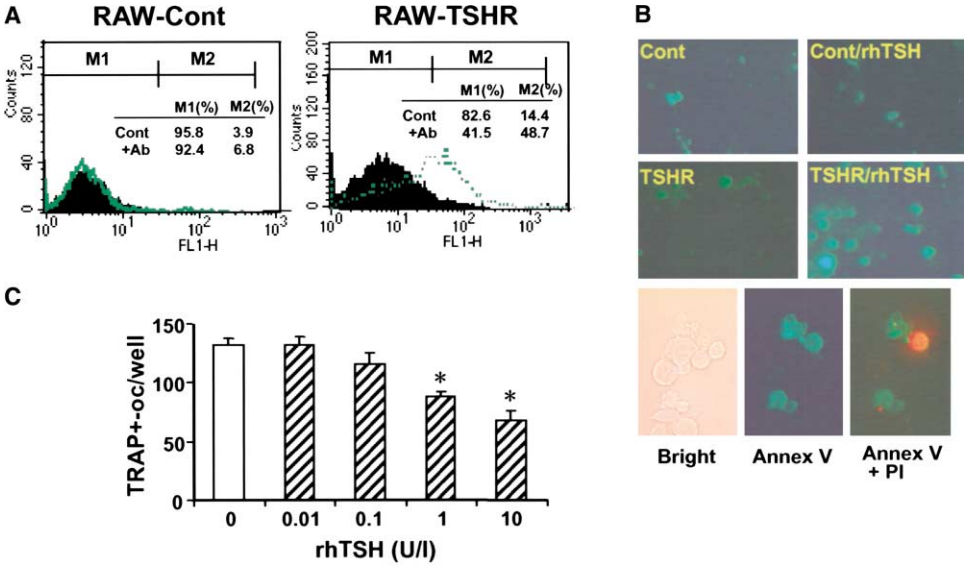

Figure 5. TSH Effects on Osteoclast and Osteoclast Precursor Survival

(A) FACS analysis to assess the expression of the TSHR in RAW264.7 cells infected with either empty pLXSN retroviral vector (RAW-Cont) or vector containing the human TSHR gene (RAW-TSHR). Percent cells in the M1 and M2 zones are indicated. Black: no added antibody; green: mouse antihuman TSHR (RSR-1) antibody (10 μg/ml) followed by goat antimouse IgG (FITC-labeled, 0.4 μg/ml). Note the spectral shift of the green zone toward M2 indicates protein expression.

(B) RAW-TSHR and RAW-Cont cells were treated with rhTSH (10 U/l) or vehicle without FBS for 6 hr. Annexin (annex) V (1 μg/ml) and propidium iodide (PI) (0.2% v/v) were applied together for 10 min, followed by fluorescence microscopy using green (annexin label) and red (PI label) filters to visualize the two fluorochromes, respectively. Note that RAW-TSHR cells, but not RAW-Cont cells displayed annexin V staining, indicating increased apoptosis resulting from TSHR activation. Minimal PI staining, indicating a generally intact cell membrane was seen with both RAW-TSHR and RAW-Cont cells.

(C) Inhibitory effect of rhTSH on the survival of mature TRAP-positive osteoclasts (oc) formed from TSHR-positive RAW-C3 cells in the presence of RANK-L (100 ng/ml). Statistics by analysis of variance; *$p < 0.01$, compared with zero concentration.

for endochondral ossification and synergizes the bone formation induced by BMP-4 (Zelzer et al., 2002; Peng et al., 2002).

TSH significantly inhibited type 1 collagen expression, as well as BSP and osteocalcin expression, respectively, in primary calvarial osteoblast (POB) and calvarial explant cultures (Figure 7C). Quite surprisingly, *Runx*-2 and osterix expression were not significantly suppressed by TSH (Figure 7D). Importantly, however, TSH profoundly inhibited LRP-5 and Flk-1 expression (Figure 7E). In parallel, the expression of both LRP-5 and Flk-1 was upregulated in $TSHR^{-/-}$ long bones compared with wild-type bones (Figure 7F). Together, the data provides compelling evidence that TSH inhibits osteoblast differentiation through a *Runx*-2- and osterix-independent mechanism involving the downregulation of the prodifferentiation factors, LRP-5 and Flk-1.

Discussion

No effects of TSH or the TSHR on bone or bone cells have ever been speculated, except for one report showing that TSH binds osteogenic sarcoma (UMR106) cell membranes (Inoue et al., 1998). It has been surmised, however, that other cells and organs including bone marrow cells, lymphocytes, the pituitary, thymus, testes, kidney, brain, adipose tissue, and fibroblasts bear functional TSHRs (for review, see Davies et al., 2002; Wang et al., 2003). However, only in two instances is the evidence for a biological role plausible. It has been suggested that TSH plays a role in recruiting specific intestinal epithelial (IE) lymphocyte subsets bearing TSHRs to the gut in response to TRH (Wang and Klein, 1995). Functional TSHRs have been demonstrated in dendritic cells and the thymus, wherein, quite curiously, the enzymatic apparatus for thyroid hormone synthesis is also present (Bagriacik and Klein, 2000). Secondly, there is evidence that TSH induces lipolysis and could thus be thermogenic (Endo et al., 1995). Preadipocytes, which arise from the same pluripotent lineage as the osteoblast, express TSHRs (Valyasevi et al., 1999). Two TSHR isoforms have been cloned from a rat adipose tissue cDNA library. The larger isoform is not detected in thyroid tissue, does not bind TSH, and fails to elicit a cAMP response (Endo et al., 1995). Thus, despite renewed interest in TSH receptor physiology, none of the suggestions for a putative role for the receptor have been tested rigorously using gain-of-function or loss-of-function strategies.

Our results show that TSHRs are of fundamental importance in skeletal conservation in adult life. This is evident from a full-blown "high remodeling" skeletal phenotype seen even when receptor levels are reduced by 50% and in the face of unimpaired thyroid function. That the remodeling defect in euthyroid heterozygotic and hypothyroid null mice is virtually indistinguishable further suggests that TSH action on bone is direct, as opposed to being secondary to reduced thyroid hormone levels. Thus, dietary thyroid extract supplementa-

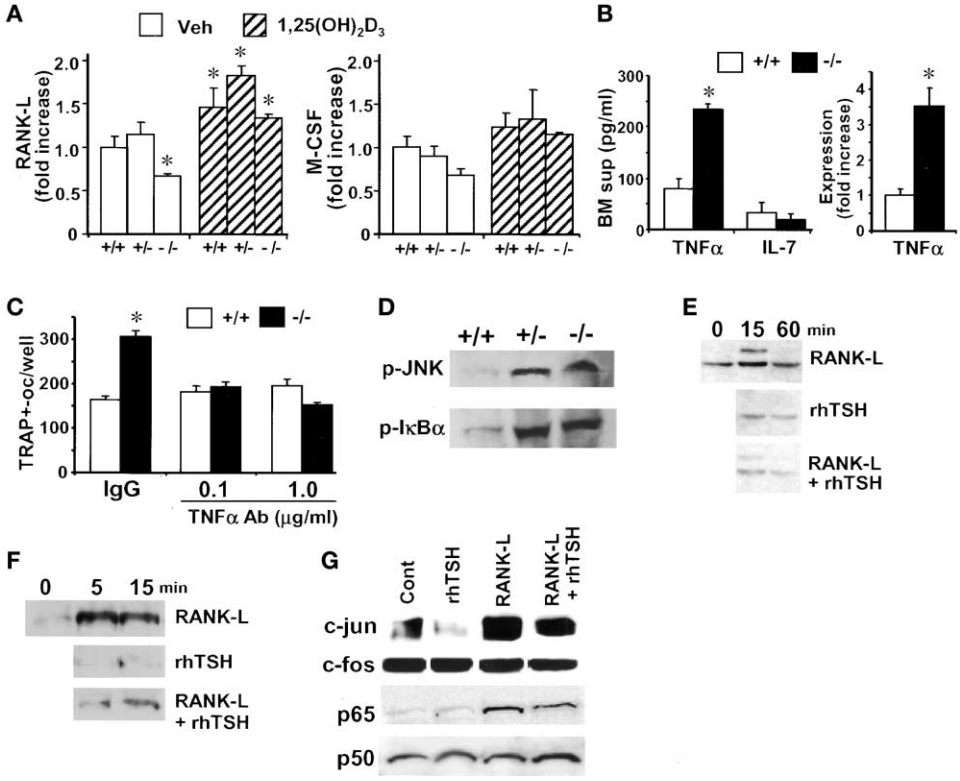

Figure 6. Mechanism of the Antiosteoclastogenic Action of TSH

(A) Real-time PCR measurements of RANK-L and M-CSF mRNA expression (fold increase) in primary osteoblasts cultured from $TSHR^{+/+}$, $TSHR^{+/-}$, and $TSHR^{-/-}$ calvaria that were incubated for 2 days in α-MEM without (Veh) or with 1,25-dihydroxyvitamin D_3 (10^{-8} M). Statistics comparing null and heterozygote with wild-type vehicle-treated cells, by analysis of variance, *$p < 0.01$.

(B) ELISA measurement of tumor necrosis factor α (TNFα) and interleukin-7 (IL-7) in the supernatant (sup) of marrow cells freshly isolated from $TSHR^{+/+}$ (+/+) and $TSHR^{-/-}$ (−/−) long bones (left image). Real-time PCR measurements for TNFα mRNA expression (fold increase) in osteoclasts derived from $TSHR^{+/+}$ (+/+) and $TSHR^{-/-}$ (−/−) bone marrow cultures (day 4) (right image). Unpaired Student's t test comparison with $TSHR^{+/+}$ bone marrow supernatants and cultured cells, respectively, $p < 0.01$ ($n = 4$ for both experiments).

(C) Effect of a neutralizing antibody to TNFα (Ab) on TRAP positive osteoclast (oc) formation following a 4 day culture (see Experimental Procedures). Comparison with $TSHR^{+/+}$ in the presence of goat antimouse IgG, $p < 0.01$.

(D) Western immunoblots showing elevated steady state levels of p-JNK and p-IκBα in osteoclasts derived from $TSHR^{+/+}$, $TSHR^{+/-}$ and $TSHR^{-/-}$ mouse bone marrow cell cultures (day 4).

(E–G) Western immunoblots on lysates prepared from RAW-C3 cells exposed to RANK-L (100 ng/ml), recombinant human (rh) TSH (10 U/l), or RANK-L (100 ng/ml) plus rhTSH (10 U/l). Phosphorylated (p) JNK (E) and p-IκBα (F) was measured in whole-cell lysates. Levels of c-*jun*, c-*fos*, and the NFκB subunits, p65 and p50, were measured in nuclear subfractions (G). Note that rhTSH inhibited basal and RANK-L stimulated JNK and IκBα phosphorylation, as well as the nuclear translocation of c-*jun* and p65, but not of c-*fos* and p50.

tion to normalize serum thyroid hormone levels failed to reverse the low BMD, calvarial thinning, or focal sclerosis.

It is interesting that TSHRs appear to modulate resorption and formation independently, a phenomenon that is undocumented for any other molecule. Normally, elevated osteoclastic resorption, for example, after gonadal steroid withdrawal, precedes and exceeds the enhanced bone formation with the primary cellular defect in ovariectomized mice being increased osteoclastogenesis (Riggs et al., 2002). However, due to the tight coupling between resorption and formation, bone formation also increases, but lags behind resorption. The overall result of such high remodeling is osteoporosis, but without focal sclerosis. Formation and resorption are not only coupled temporally, but also spatially, so that each resorptive cavity must be refilled with new bone to maintain skeletal integrity. That TSHR knockout mice have focal sclerosis in addition to high remodeling osteoporosis suggests that osteoblastic activity, as in Pagetic bone, is pronounced, autonomous, and, at least in part, dissociated spatially from resorption. Thus, bone formation appears to occur "ectopically" at sites that have not been previously resorbed, resulting in a focal sclerotic phenotype accompanying global osteopenia. This is consistent with our demonstration that (1) the in vitro effects of TSH are exerted separately on osteoblast and osteoclast precursors; (2) TSHRs are present on both cell types; and (3) the osteoclastic phenotype does not result from enhanced RANK-L and M-CSF expression in osteoblasts.

TSH thus inhibits osteoclastogenesis and osteoblastogenesis through distinct and unrelated mechanisms. It acts on TSHR-bearing osteoclast precursors to inhibit JNK phosphorylation and the subsequent nuclear translocation of the transcription factor c-*jun*. Although we have not tested this directly, reduced c-*jun* levels, even in the face of unaltered c-*fos* levels, will result in reduced

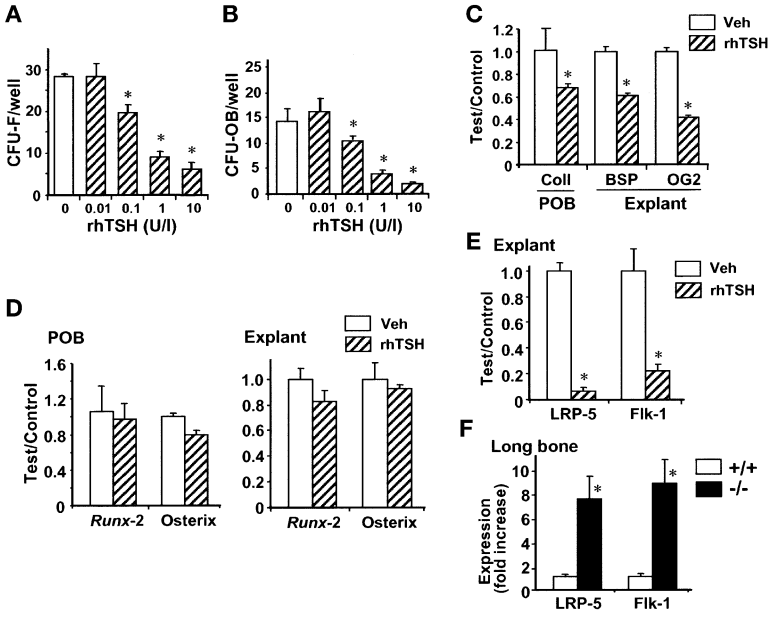

Figure 7. TSH Effects on Osteoblast Formation

Inhibitory effect of recombinant human (rh) TSH on the formation of colony forming unit-fibroblasts (CFU-F) (A) and CFU-osteoblasts (CFU-OB) (B). Stromal cells were allowed to differentiate in ascorbic acid-2-phosphate (1 mM). Within 10 days, adherent fibroblastoid colonies, CFU-Fs, formed that stained positive for alkaline phosphatase. These colonies, upon further incubation, mineralized around 21 days to form CFU-OBs that were identifiable upon brownish black von Kossa staining. Statistics by analysis of variance, comparison with zero dose of rhTSH, $p < 0.01$.

(C–E) Expression levels (test/control), determined by real-time PCR of type 1 collagen (coll), bone sialoprotein (BSP), osteocalcin (OG2) (C), *Runx-2* and osterix (D), as well as LRP-5 and Flk-1 (E) in either primary calvarial osteoblasts (POB) or primary calvarial explant cultures (Explant) in response to rhTSH (10 U/l) or vehicle (Veh).

(F) Elevated expression, determined by real-time PCR (as above), of LRP-5 and Flk-1 in long bones of $TSHR^{-/-}$ and $TSH^{+/-}$ compared with wild-type littermates. Statistics by analysis of variance, *$p < 0.01$, comparing either to zero concentration (A–E) or to wild-type cells (F).

homo- and heterodimer formation, and hence, diminish the transcription of critical osteoclast target genes bearing AP-1 sites, such as TRAP and cathepsin K (Kawaida et al., 2003). An identical mechanism transduces the antiosteoclastogenic effect of estrogen (Shevde et al., 2000; Srivastava et al., 2001). In contrast to estrogen, however, TSH additionally inhibits IκBα phosphorylation. This makes more dephosphorylated IκBα available to bind to and hence prevent the nuclear translocation of NFκB heterodimers. Interestingly, we found that the translocation of p65 (and not of p50) was inhibited selectively in response to TSH. NFκB, the absence of which results in osteopetrosis without osteoclasts (Iotsova et al., 1997), regulates the transcription of a variety of genes during osteoclastogenesis, including ICAM, TLR2, and IκBα itself (Wei et al., 2001). It is highly likely therefore that the two mechanisms, JNK/*c-jun* and NFκB, acting in concert are responsible for the profound inhibitory effects of TSH on osteoclast formation.

The physiological relevance of both mechanisms was confirmed ex vivo by the marked enhancement of JNK and IκBα phosphorylation seen in cells derived from $TSH^{-/-}$ and $TSH^{+/-}$ mice. JNK and IκBα are both phosphorylated in response to TNFα that regulates osteoclast formation (Lam et al., 2000). Our finding that the expression of TNFα is enhanced dramatically in vivo and that a neutralizing anti-TNFα antibody inhibits the enhanced osteoclastogenesis ex vivo in $TSHR^{-/-}$ bone marrow cell cultures suggests TNFα as a proosteoclastic signal mediating the effects of TSHR deletion.

The effect of TSH in negatively regulating osteoblast formation is independent of both *Runx-2* and osterix. We found that the expression of LRP-5, the Wnt coreceptor, and Flk-1, a VEGF receptor, were reduced dramatically in response to TSH both in primary osteoblasts and explant cultures. Likewise, receptor expression was upregulated in $TSH^{-/-}$ mice that had enhanced bone formation and focal sclerosis. Mutations of the LRP-5 gene in humans or its targeted disruption in the mouse result in osteopenia; in the latter case, *Runx*-2 expression remains normal (Kato et al., 2002). Thus, our result that TSH exerts an effect by inhibiting LRP-5 independently of *Runx-2* comes as no surprise. We are, however, less clear on the mechanism through which Flk-1 mediates TSH effects on osteoblastogenesis, except that there is evidence that VEGF can, through Flk-1 activation, synergize the actions of BMP-4 (Peng et al., 2002). The latter effect likely occurs through the enhancement of mesenchymal cell proliferation.

Finally, it is tempting to speculate that the skeletal loss that occurs in hyperthyroidism is due to low TSH levels as opposed solely to high T_3 and T_4 levels. If so, this would mean revisiting the mechanism of bone loss in thyroid disease, particularly in patients on thyroxine therapy. On one hand, there is substantive early literature on direct stimulatory effects of thyroid hormone on osteoblasts and osteoclasts (Bordier et al., 1967; Sato et al., 1987; Britto et al., 1994). On the other hand, mice rendered null for the α1 and β thyroid hormone receptors (TRs) do not exhibit any bone remodeling defects (Gothe et al., 1999). $TR\alpha1^{-/-}\beta^{-/-}$ mice instead have abnormalities in skeletal maturation characterized by severe runting and growth plate defects. These features are recapitulated only in hypothyroid $TSHR^{-/-}$ mice, not in euthyroid $TSHR^{+/-}$ mice that have a profound remodeling phenotype. Moreover, only the maturation defect and not the remodeling defect in $TSHR^{-/-}$ mice is reversed by thyroid replacement. The studies thus make a compelling argument for the regulation of bone remodeling by TSH and the TSHR, and of skeletal morphogenesis by thyroid

hormones. With the recent discovery of RANK-L and osteoprotegerin expression in thyroid follicles (Hofbauer et al., 2002), it becomes tempting to speculate that the thyroid gland might regulate skeletal morphogenesis and remodeling in unusual ways that require further investigation.

Experimental Procedures

Specialized Culture Techniques

For the osteoclastogenesis experiments, bone marrow cells were isolated from femora and tibiae of mice in α-MEM. The cells were cultured for 2 days with M-CSF (5 ng/ml). Nonadherent cells were collected and purified by Ficoll-Plus (Amersham Pharmacia Biotech Inc., Arlington Height, IL). The cells were then incubated with M-CSF (30 ng/ml) and RANK-L (60 ng/ml) for 4–6 days followed by their staining for TRAP using a kit (Sigma) per manufacturer's instruction. The number of TRAP-positive cells was counted. RAW-C3 cells were cultured with RANK-L (10–100 ng/ml) for 3 days to form TRAP-positive osteoclasts. For osteoclast survival experiments, the cells were cultured with RANK-L (100 ng/ml) for 3 days and then with RANK-L (10 ng/ml) and rhTSH (10 U/l) for an additional 3 days. In separate experiments, a neutralizing polyclonal goat antimouse TNFα antibody (R&D Systems Inc., Minneapolis, MN) was added at 0.1 and 1.0 μg/ml at day zero. Preimmune goat IgG was used as control.

For osteoblastogenesis experiments, bone marrow cells were cultured in the presence of ascorbic acid-2-phosphate (1 mM). At around 3 days, multicellular fibroblastoid colonies, CFU-Fs, appeared that became increasingly alkaline phosphatase positive over the following week. CFU-F colonies were stained for alkaline phosphatase using a kit per manufacturer's recommendations (Sigma-Aldrich, St. Louis, MO). Upon further incubation, the colonies mineralized to form CFU-osteoblast (CFU-OB) that stained brownish black with von Kossa. CFU-F and CFU-OB numbers were determined (Abe et al., 2000; Sun et al., 2003).

For primary osteoblast cultures, calvaria from 4-day-old mice were dissected and digested five times in sequence with collagenase (0.2% w/v) for 10 min each time. Fractions 2 to 5 were pooled and cultured for 3 days in α-MEM for amplification, followed by differentiation in ascorbic acid-2-phosphate (1 mM). For explant cultures, 1-day-old calvaria were maintained for 6 days in α-MEM containing ascorbic acid-2-phosphate (1 mM).

Bone Phenotyping

BMD measurements were performed on anaesthetized mice using a Lunar Piximus with an error of $<1.5\%$. Whole-body BMD (with the cranium excluded) and region-specific measurements, notably of the spine (L4–L6), right and left femur, and right and left tibia were made. The instrument was calibrated each time before use by employing a phantom per manufacturer's recommendation. In addition, microradiography and polarized microscopy were used to examine for radioopacities and collagen orientation, respectively.

The mice were then sacrificed per our IACUC approved protocol. The vertebral column, femur, and tibia were cleaned of excess muscle and soft tissue and processed for histological examination. The bones were placed overnight in phosphate-buffered paraformaldehyde (5%, v/v), were then decalcified with HCl, dehydrated, and embedded in paraffin. 6 μm sections were cut and stained with hematoxylin and eosin. In separate experiments, double-calcein labeling was carried out to examine the extent and rate of osteoblastic bone formation. Calcein, 10 mg/kg body weight, was administered subcutaneously on days −7 and −2. The mice were sacrificed on day 0, and long bones were immersed in OCT compound (Sakura Finetechnical Co. Tokyo, Japan) and frozen in liquid nitrogen. 6 μm frozen sections were cut using a Reichert-Jung sledge microtome. The calcein labels were examined using a 380–425 nm excitation filter and a 450 nm emission filter.

TSHR Immunodetection and ^{125}I-TSH Binding

TSHR expression in heterozygote mice was established by examining GFP fluorescence in bone or bone marrow-derived osteoclast and osteoblast precursors by conventional epifluorescence microscopy complemented by dual photon confocal imaging or immunodetection. In addition, FACS was used to (1) demonstrate TSHR in wild-type osteoblast and osteoclast precursors, including TSHR-positive RAW-C3 cells, and (2) to check for TSHR expression in RAW264.7 cells that had been infected with a retrovirus containing the human TSHR gene (RAW-TSHR) or with empty vector (RAW-control). A mouse monoclonal antihuman TSHR antibody, RSR-1 (epitope: amino acids 381 to 385, β subunit) was employed. Cells were incubated with RSR-1 (10 μg/ml, 1 hr) followed by a goat antimouse IgG (FITC-labeled) (0.4 μg/ml, 1 hr). For immunodetection of TSHR, RANK, and calcitonin receptor during osteoclastogenesis, monoclonal (RSR-1) or polyclonal (antimouse RANK and CTR) antibodies (Santa Cruz Biotechnology Inc., Santa Cruz, CA) were applied to bone marrow cells that had been incubated for 2–4 days in RANK-L (60 ng/ml) and M-CSF (30 ng/ml).

For binding studies, RAW-C3 cells were washed with modified Hanks' solution and incubated in modified Hanks' solution with ^{125}I-bTSH (10,000 cpm/well) and bovine TSH (10^6 mU/l) for 2 hr at 37°C in 96-well plates (Ando et al., 2002). Radioactivity of the cell lysate was measured after washing. As negative and positive controls, CHO cells were transfected, respectively, with empty vector or human or murine TSHR (Ando et al., 2002).

For immunodetection of signaling molecules, namely Erk1/2, p38, Akt, JNK, IκBα, p65, p50, c-*jun*, and c-*fos*, Western immunoblotting was performed on whole-cell lysates and nuclear subfractions obtained as described previously (Shevde et al., 2000). The respective antibodies were obtained from Santa Cruz Biotechnology Inc. (Santa Cruz, CA) or Cell Signaling Technology, Inc. (Beverly, MA).

Bone marrow was collected from long bones dissected from TSHR$^{-/-}$ and TSHR$^{+/+}$ mice and suspended in 1 ml α-MEM. After obtaining total cell counts, the suspension was centrifuged at 2000 rpm for 5 min and the supernatant separated. ELISAs for TNFα and IL-7 were performed on supernatants using capture and detection antibodies for the two cytokines obtained from Pharmigen (San Diego, CA) and R&D Systems Inc., respectively. The assay was established and optimized per manufacturer's instruction.

Real-Time PCR

Total RNA was purified using RNeasy Mini kit (Qiagen, Valencia, CA) per manufacturer's protocol. Expression levels of various transcripts were determined by quantitative real-time RT-PCR. Briefly, 5.0 μg total RNA was converted into cDNA using by Superscript II (Invitrogen, Carlsbad, CA) and 1/200 (∼500 pg) was utilized for 40 cycle two-step PCR in an ABI Prism 7000 (Applied Biosystems, Foster City, CA) in SYBR Green Master Mix (ABI) and 200 nM primers. Amplicon size and reaction specificity was confirmed by agarose gel electrophoresis. Each transcript in each sample was assayed 3 times and the fold-change ratios between experimental and control samples for each gene used in the analysis were calculated.

Acknowledgments

The studies were supported by grants from the National Institutes for Health (AG-14917-8 and AG23176-01 to M.Z.; and DK52464, DK45011, and A124671 to T.F.D.). E.A. and M.Z. also thank the Department of Veterans Affairs for support (GRECC and Merit Review Awards to M.Z. and E.A.). The authors acknowledge with gratitude critical comments and generous advice from Professors Iain MacIntyre, FRS (University of London); Christopher L.-H. Huang, MD, PhD (University of Cambridge); Gerard Karsenty, MD, PhD (Baylor College of Medicine); and F. Patrick Ross, PhD (Washington University of St. Louis). M.Z. thanks Mary Jo Sweeney, BS, for expert assistance in preparing the manuscript. R.M. thanks support from the National Institutes for Health (DK07646).

Received: November 26, 2002
Revised: September 10, 2003
Accepted: September 16, 2003
Published: October 16, 2003

References

Abe, E., Yamamoto, M., Taguchi, Y., Lecka-Czernik, B., O'Brien, C.A., Economides, A.N., Stahl, N., Jilka, R.L., and Manolagas, S.C.

(2000). Essential requirement of BMPs-2/4 for both osteoblast and osteoclast formation in murine bone marrow cultures from adult mice: antagonism by noggin. J. Bone Miner. Res. *4*, 663–673.

Ando, T., Lauf, R., Moran, T., Nagayama, Y., and Davies, T.F. (2002). A monoclonal thyroid-stimulating antibody. J. Clin. Invest. *110*, 1667–1674.

Bagriacik, E.U., and Klein, J.R. (2000). The thyrotropin (thyroid-stimulating hormone) receptor is expressed on murine dendritic cells and on a subset of CD45RB high lymph node T cells: functional role for thyroid-stimulating hormone during immune activation. J. Immunol. *164*, 6158–6165.

Blair, H.C., Zaidi, M., and Schlesinger, P.H. (2002). Mechanisms balancing skeletal matrix synthesis and degradation. Biochem. J. *364*, 329–341.

Bordier, P., Miravet, L., Matrajt, H., Hioco, D., and Ryckewaert, A. (1967). Bone changes in adult patients with abnormal thyroid function (with special reference to ^{45}Ca kinetics and quantitative histology). Proc. R. Soc. Med. *60*, 1132–1134.

Britto, J.M., Fenton, A.J., Holloway, W.R., and Nicholson, G.C. (1994). Osteoblasts mediate thyroid hormone stimulation of osteoclastic bone resorption. Endocrinology *134*, 169–176.

Davies, T.F., Marians, R., and Latif, R. (2002). The TSH receptor reveals itself. J. Clin. Invest. *110*, 161–164.

Endo, T., Ohta, K., Haraguchi, K., and Onaya, T. (1995). Cloning and functional expression of a thyrotropin receptor cDNA from rat fat cells. J. Biol. Chem. *270*, 10833–10837.

Gong, Y., Slee, R.B., Fukai, N., Rawadi, G., Roman-Roman, G., Reginato, A.M., Wang, H., Cundy, T., Glorieux, F.H., Lev, D. et al. (2001). LDL receptor-related protein 5 (LRP5) affects bone accrual and eye development. Cell *107*, 513–523.

Gothe, S., Wang, Z., Ng, L., Kindblomm, J.M., Barrosm, A.C., Ohlssonm, C., Vennstrom, B., and Forrest, D. (1999). Mice devoid of all known thyroid hormone receptors are viable but exhibit disorders of the pituitary-thyroid axis, growth, and bone maturation. Genes Dev. *13*, 1329–1341.

Greenspan, S.L., and Greenspan, F.S. (1999). The effect of thyroid hormone on skeletal integrity. Ann. Intern. Med. *130*, 750–758.

Hofbauer, L.C., Kluger, S., Kuhne, C.A., Dunstan, C.R., Burchert, A., Schoppet, M., Zielke, A., and Heufelder, A.E. (2002). Detection and characterization of RANK ligand and osteoprotegerin in the thyroid gland. J. Cell. Biochem. *86*, 642–650.

Inoue, M., Tawata, M., Yokomori, N., Endo, T., and Onaya, T. (1998). Expression of thyrotropin receptor on clonal osteoblast-like rat osteosarcoma cells. Thyroid *8*, 1059–1064.

Iotsova, V., Caamano, J., Loy, J., Yang, Y., Lewin, A., and Bravo, R. (1997). Osteopetrosis in mice lacking NF-kappaB1 and NF-kappaB2. Nat. Med. *3*, 1285–1289.

Karsenty, G., and Wagner, E.F. (2002). Reaching a genetic and molecular understanding of skeletal development. Dev. Cell *2*, 389–406.

Kato, M., Patel, M.S., Levasseur, R., Lobov, I., Chang, B.H.-J., Glass, D.A., II, Hartmann, C., Li, L., Hwang, T.-H., Brayton, C.F., et al. (2002). Cbfa1-independent decrease in osteoblast proliferation, osteopenia, and persistent embryonic eye vascularization in mice deficient in Lrp5, a Wnt coreceptor. J. Cell Biol. *157*, 303–314.

Kawaida, R., Ohtsuka, T., Jokutsu, J., Takahashi, T., Kadono, Y., Oda, H., Hikita, A., Nakamura, K., Tanaka, S., and Furukawa, H. (2003). Jun dimerization protein 2 (JDP2), a member of the AP-1 family of transcription factor, mediates osteoclast differentiation induced by RANKL. J. Exp. Med. *197*, 1029–1035.

Khosla, S. (2001). Minireview: the OPG/RANKL/RANK system. Endocrinology *142*, 5050–5055.

Kohn, L.D., Shimura, H., Shimura, Y., Hidaka, A., Giuliani, C., Napolitano, G., Ohmori, M., Laglia, G., and Saji, M. (1995). The thyrotropin receptor. Vitam. Horm. *50*, 287–384.

Lam, J., Takeshita, S., Barker, J.E., Kanagawa, O., Ross, F.P., and Teiterbaum, S.L. (2000). TNF-α induces osteoclastogenesis by direct stimulation of macrophage exposed to permissive levels of RANK ligand. J. Clin. Invest. *106*, 1481–1488.

Lecka-Czernik, B., Gubrij, I., Moerman, E.J., Kajkenova, O., Lipschitz, D.A., Manolagas, S.C., and Jilka, R.L. (1999). Inhibition of Osf2/Cbfa1 expression and terminal osteoblast differentiation by PPARgamma2. J. Cell. Biochem. *74*, 357–371.

Manolagas, S.C., and Jilka, R.L. (1995). Bone marrow, cytokines, and bone remodeling. Emerging insights into the pathophysiology of osteoporosis. N. Engl. J. Med. *332*, 305–311.

Marians, R.C., Ng, L., Blair, H.C., Unger, P., Graves, P.N., and Davies, T.F. (2002). Defining TSH-dependent and TSH-independent steps of thyroid hormone synthesis using thyrotropin receptor-null mice. Proc. Natl. Acad. Sci. USA *99*, 15776–15781.

Parfitt, A.M., Drezner, M.K., Glorieux, F.H., Kanis, J.A., Malluche, H., Meunier, P.J., Ott, S.M., and Recker, R. (1987). Bone histomorphometry: standardization of nomenclature, symbols, and units. J. Bone Miner. Res. *2*, 595–610.

Peng, H., Wright, V., Usas, A., Gearhart, B., Shen, H.-C., Cummins, J., and Huard, J. (2002). Synergistic enhancement of bone formation and healing by stem cell-expressed VEGF and bone morphogenetic protein-4. J. Clin. Invest. *110*, 751–759.

Prummel, M.F., Brokken, L.J., Meduri, G., Misrahi, M., Bakker, O., and Wiersinga, W.M. (2000). Expression of the thyroid-stimulating hormone receptor in the folliculo-stellate cells of the human anterior pituitary. J. Clin. Endocrinol. Metab. *85*, 4347–4353.

Riggs, B.L., Khosla, S., and Melton, L.J. (2002). Sex steroids and the construction and conservation of the adult skeleton. Endocr. Rev. *3*, 279–302.

Sato, K., Han, D.C., Fujii, Y., Tsushima, T., and Shizume, K. (1987). Thyroid hormone stimulates alkaline phosphatase activity in cultured rat osteoblastic cells (ROS 17/2.8) through 3,5,3′-triiodo-L-thyronine nuclear receptors. Endocrinology *120*, 1873–1881.

Shevde, N.K., Bendixen, A.C., Dienger, K.M., and Pike, J.W. (2000). Estrogens suppress RANK ligand-induced osteoclast differentiation via a stromal cell independent mechanism involving c-Jun repression. Proc. Natl. Acad. Sci. USA *97*, 7829–7834.

Sims, N.A., Clement-Lacroix, P., Minet, D., Fraslon-Vanhulle, C., Gaillard-Kelly, M., Resche-Rigon, M., and Baron, R. (2003). A functional androgen receptor is not sufficient to allow estradiol to protect bone after gonadectomy in estradiol receptor-deficient mice. J. Clin. Invest. *111*, 1319–1327.

Sun, L., Iqbal, J., Dolgilevich, S., Yuen, T., Wu, X.B., Moonga, B.S., Adebanjo, O.A., Bevis, P.J., Lund, F., Huang, C.L., et al. (2003). Disordered osteoclast formation and function in a CD38 (ADP-ribosyl cyclase)-deficient mouse establishes an essential role for CD38 in bone resorption. FASEB J. *17*, 369–375.

Srivastava, S., Toraldo, G., Weitzmann, M.N., Cenci, S., Ross, F.P., and Pacifici, R. (2001). Estrogen decreases osteoclast formation by down-regulating receptor activator of NF-kappa B ligand (RANKL)-induced JNK activation. J. Biol. Chem. *276*, 8836–8840.

Takahashi, N., Udagawa, N., Tanaka, S., and Suda, T. (2003). Generating murine osteoclasts from bone marrow. Methods Mol. Med. *80*, 129–144.

Teitelbaum, S.L., and Ross, F.P. (2003). Genetic regulation of osteoclast development and function. Nat. Rev. Genet. *4*, 638–649.

Valyasevi, R.W., Erickson, D.Z., Harteneck, D.A., Dutton, C.M., Heufelder, A.E., Jyonouchi, S.C., and Bahn, R.S. (1999). Differentiation of human orbital preadipocyte fibroblasts induces expression of functional thyrotropin receptor. J. Clin. Endocrinol. Metab. *84*, 2557–2562.

Vincent, B.L., O'Donoghue, A.J., Glimcher, M.J., and McHugh, K.P. (2001). RAW264 cell clones are transcriptional osteoclast precursors. J. Bone Miner. Res. S268.

Wang, H.-C., Dragoo, J., Zhou, Q., and Klein, J.R. (2003). An intrinsic thyrotropin-mediated pathway of TNF$-\alpha$ production by bone marrow cells. Blood *101*, 119–123.

Wang, J., and Klein, J.R. (1995). Hormonal regulation of extrathymic gut T cell development: involvement of thyroid stimulating hormone. Cell. Immunol. *161*, 299–302.

Webber, D.M., Braidman, I.P., Robertson, W.R., and Anderson, D.C. (1988). A quantitative cytochemical assay for osteoclast acid phosphatase activity in foetal rat calvaria. Histochem. J. *20*, 269–275.

Wei, S., Teitelbaum, S.L., Wang, M.W., and Ross, F.P. (2001). Receptor activator of nuclear factor-kappa B ligand activated nuclear factor-kappa B in osteoclasts. Endocrinology *142*, 1290–1295.

Zaidi, M., Blair, H.C., Abe, E., Moonga, B.S., and Huang, C.L.-H. (2003). Osteoclastogenesis, bone resorption and osteoclast-based therapeutics. J. Bone Miner. Res. *18*, 599–609.

Zelzer, E., McLean, W., Ng, Y.-S., Fukai, N., Reginato, A.M., Lovejoy, S., D'Amore, P.A., and Olsen, B.R. (2002). Skeletal defects in $VEGF^{120/120}$ mice reveal multiple roles for VEGF in skeletogenesis. Development *129*, 1893–1904.